Sinop Üniversitesi Fen Bilimleri Dergisi *Sinop Uni J Nat Sci 2(1): 37 - 47 (2017)*
ISSN: **2536-4383**

Research Article

Synthesis of Hydroxyapatite-alginate Composite: Methylene Blue Adsorption

Tebriz Aslanov [a], ***Deniz Uzunoğlu*** [a*], ***Ayla Özer*** [a]

[a] *Mersin University, Chemical Engineering Department, Mersin, Turkey*

Abstract

In this study, hydroxyapatite-alginate (HAp-SA) composite spheres were synthesized and characterized and then the methylene blue dyestuff (MB) removal was investigated by using the synthesized HAp-SA composite spheres as adsorbent. The effects of environmental conditions for MB adsorption onto HAp-SA composite spheres were investigated and the optimum environmental conditions were obtained as follows: initial pH of 9.0, initial dye concentration of 300 mg L^{-1}, temperature of 25 °C, and adsorbent concentration of 1.0 g L^{-1}. At the optimum conditions; the MB adsorption capacities of HAp-SA spheres, HAp-SA films, alginate spheres and HAp were compared to interpret the effectiveness of the synthesized composite materials. Besides, the multistage adsorption system was also investigated for the adsorption of MB onto the synthesized HAp-SA composite spheres. Moreover, the adsorption equilibrium and thermodynamic parameters were also determined.

Keywords: Adsorption, adsorbent characterization, composite materials, dye removal

Hidroksiapatit-Aljinat Kompozitlerinin Sentezi: Metilen Mavisi Adsorpsiyonu

Öz

Bu çalışmada, hidroksiapatit-aljinat (HAp-SA) kompozit küreleri sentezlendi ve karakterizasyonu yapıldı, daha sonra bunlar metilen mavisi boyarmaddesi (MB)'nin adsorpsiyonunda adsorbent olarak kullanıldı. MB'nin HAp-SA kompozit kürelerine adsorpsiyonuna çevresel koşulların etkisi araştırıldı ve optimum başlangıç pH'sı, boyarmadde derişimi, sıcaklık ve adsorbent derişimi sırasıyla 9.0, 300 mg L^{-1}, 25 °C ve 1.0 g L^{-1} olarak belirlendi. Ayrıca, sentezlenen kompozit malzemelerin verimliliklerini yorumlamak amacıyla belirlenen optimum ortam koşullarında; HAp-SA kompozit kürelerinin, HAp-SA kompozit filmlerinin, SA kürelerinin ve HAp'nin MB'yi adsorplama kapasiteleri karşılaştırıldı. Buna ek olarak, MB'nin HAp-SA kompozit kürelerine adsorpsiyonu için çok kademeli adsorpsiyon sistemi araştırıldı. Ayrıca, adsorpsiyon denge ve termodinamik parametreleri de belirlendi.

Anahtar Kelimeler: Adsorpsiyon, adsorbent karakterizasyonu, boyarmadde giderimi, kompozit malzeme

---

[*] Corresponding author:
e-mail: denizuzunoglu4@gmail.com

Received: 24.11.2016
Accepted: 16.02.2017

Introduction

There are many investigations on physicochemical/biological methods of treating colorful effluents, such as oxidation, coagulation/flocculation, electrochemical treatment, ultrafiltration, aerobic/anaerobic method, and adsorption/biosorption. Production of secondary sludge, high capital and operational cost, sensitive operating conditions, and low efficiency are some limitations of most of these treatment methods [1]. Among these methods; adsorption using low-cost and eco-friendly adsorbent arouses attention due to its being economic and efficient for removing colorful effluents. Thus various researchers have focused on the synthesis/preparation of new low-cost, eco-friendly, and efficient adsorbents by usage of natural/biological materials or industrial wastes. Recently, the studies about the synthesis/preparation of inorganic composites supported biopolymer has increased due to their unique structure and properties. The mechanical properties of the composites can be improved with the aid of the synergistic effect of inorganic material and biopolymer [2]. Sodium alginate (SA) is a natural linear polysaccharide, non-toxic, hydrocolloids, water-soluble, and biodegradable biopolymer which is widely used as a gelling agent of binder for preparing various composite materials because SA can form gel with divalent cations such as calcium under mild conditions. The application of SA in wastewater treatment is limited due to its tendency to swell in water and other mechanical weakness [3]. In this respect, it can be blended with hydroxyapatite (HAp), inorganic material, in order to overcome the disadvantages of alginate and to gather the good properties of both materials. In this study, both sphere and film forms of alginate- hydroxyapatite composite materials were synthesized and these composite adsorbents were used for the methylene blue (MB) removal. The effects of different environmental conditions were investigated. Also, at the optimum conditions; the MB adsorption capacities of HAp-SA spheres, HAp-SA films, alginate spheres and HAp were compared to interpret the effectiveness of composite materials. Equilibrium and mass transfer modeling, thermodynamic and also adsorbent characterization studies were carried out.

Materials and Methods

Preparation of HAp-SA composite materials

0.6 g of HAp was stirred in 60 mL distilled water for 60 min, and then it was sonicated for 10 min because the particles extremely tended to agglomerate in water. In order to attain homogeneous and fine dispersion, afore-mentioned cycle was repeated once more. Then, 0.6 g of SA was added to the prepared HAp solution. To obtain a homogeneous mixture, the resulting HAp-SA solution was stirred magnetically at 1400 rpm for 6.0 h. The final mixture was dropped by syringe pump into 0.1 mole L^{-1} of $CaCl_2$ and the solution was stirred slowly for 2.0 h. The prepared spheres were washed with pure water and were dried overnight in a stove at 60 °C. For preparing composite films, filter papers were cut and immersed into the HAp-SA mixture. By this way, HAp-SA mixture was absorbed on the filter paper surface. Next, the saturated filter papers were put into 0.1 mole L^{-1} $CaCl_2$ solution and stirred slowly for 2 h. The treated filter papers were washed with pure water and were dried overnight in a stove at 60 °C. The resulting composite films were recovered from filter papers. The prepared composite materials were stored at +4 ^{o}C in the refrigerator [4].

Adsorption Studies

The effects of experimental conditions on MB adsorption onto HAp-SA spheres such as initial pH, initial dye concentration, temperature, and adsorbent concentration were investigated in a batch mode. For this purpose, the desired amount of HAp-SA spheres was mixed with 100 ml of the required initial pH and initial dye concentration in conical flasks. The conical flasks were shaken in a water bath at constant temperature for 5 h to obtain the adsorption equilibrium. At pre-determined time intervals (0, 0.5, 2.0, 5.0, 10, 20, 30, 60, 120, 180, 240, and 300 min), the sample solutions of MB were taken and separated from HAp-SA spheres with centrifuge at 4000 rev min^{-1} for 3 min, and the residual MB concentration in the supernatant was analyzed at 665 nm with Chebios brand UV–vis spectrophotometer.

Results and Discussion

Effect of environmental conditions

The single stage adsorption of MB onto HAp-SA spheres was investigated in a batch process as a function of initial pH, initial dye concentration, adsorbent concentration, and temperature.

Effect of initial pH

The effect of initial pH is the most important parameter for the adsorption processes. The variation of MB adsorption on HAp-SA spheres with initial pH was shown in Fig. 1. As can be seen from Fig. 1; the maximum adsorbed MB amount at equilibrium was obtained at initial pH 9.0, and high adsorption capacities were also obtained in the wide pH range. It can be explained with the surface charges of HAp-SA spheres. It is estimated that the surface charges of HAp-SA spheres in the pH range are negatively charged that can easily interact with the positively charged MB and eventually cause high MB adsorption. So, the optimum initial pH was determined as 9.0.

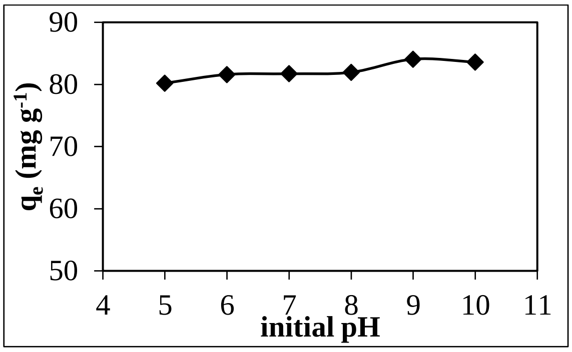

Fig 1. *Effect of initial pH*

Effect of initial MB concentration and contact time

Variation of the adsorption data of MB on HAp-SA spheres for the initial dye concentrations with time is given in Fig. 2. As indicated by the plateau of the data in Fig. 2; generally, MB adsorption was fast initially and then the adsorption was gradual and ultimately obtained saturation at equilibrium [5].

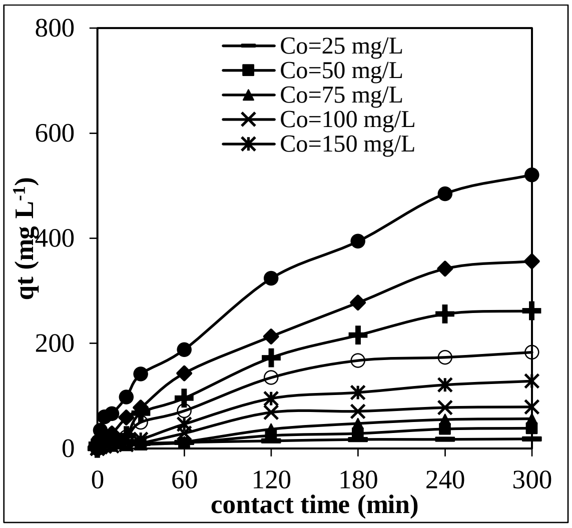

Fig 2. *Effect of initial dye concentration*

According to Fig. 2, MB adsorption increased with increasing contact time down to 180 min for the initial MB concentration range of 25-200 mg/L while it was 300 min for the higher initial dye concentrations. After these equilibrium times, the adsorbed amounts remained almost constant as a result of to be covered sites with the dye cations [5]. Therefore, it is concluded that 300 min is an adequate contact time to achieve MB adsorption equilibrium. This may stem from the saturation of the active adsorption sites of HAp-SA spheres at higher MB concentration.

Effect of adsorbent concentration

The adsorption studies of MB onto HAp-SA spheres was carried out by diversifying the adsorbent concentration 0.1- 4.0 g L^{-1}. Fig. 3 shows the plot of equilibrium adsorbed amounts (mg g^{-1}) and dye removal efficiencies (%) against adsorbent concentrations (g L^{-1}). As understood from Fig. 3; the equilibrium adsorbed amounts diminished with increasing adsorbent concentration, but the adsorption percentages increased up to 1.0 g L^{-1} of the adsorbent concentration, and then almost remained constant with farther increasing adsorbent concentration; so the optimum adsorbent concentration was obtained as 1.0 g L^{-1}. The increase in adsorbent concentration facilitates to increase the surface area and also the number of active adsorption sites; thus, the adsorption percentages increase in this way. The reason of the decreasing adsorbed amounts may be availability of utilizing of the active adsorption sites; i.e., all active adsorption sites are completely exploited at lower adsorbent concentration while only part of active adsorption sites are occupied by dye cations at higher adsorbent concentration.

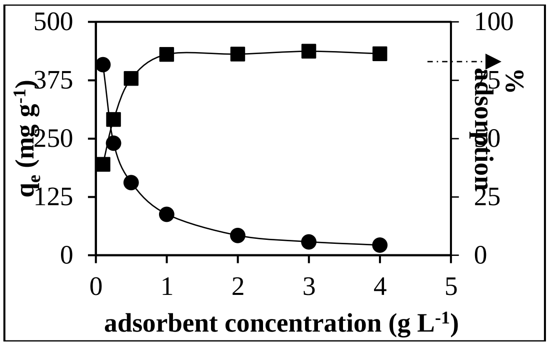

Fig 3. *Effect of adsorbent concentration*

Effect of temperature

The batch adsorption study was performed at 20, 25, 40, and 60 °C to ascertain the effect of temperature on MB adsorption; and the results were exhibited in Fig. 6. According to Fig. 4; the equilibrium uptake amounts increased in the range of 20-25 °C as a result of the increase in the motility of MB cations and also increase in the number of available active surface sites on HAp-SA spheres for adsorption in consequence of pore enlargement. The adsorbed amounts at equilibrium diminished with increase in temperature at temperature values higher than 25 °C due to its exothermic in nature. So the optimum temperature was determined as 25°C.

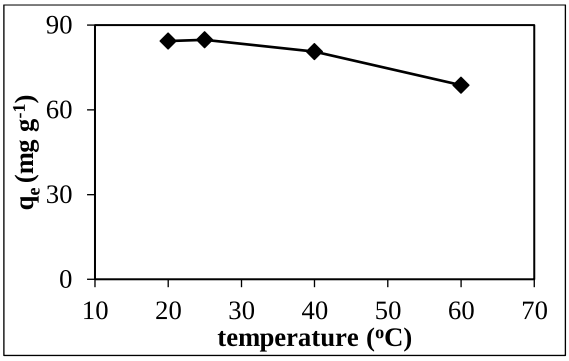

Fig 4. *Effect of temperature*

Besides, the thermodynamic parameters like Gibbs free energy ($\Delta G = -RT.\ln K_c$), enthalpy (ΔH) and entropy (ΔS) were calculated by using Van't Hoff equation ($\ln K_c = [\Delta S/R] - [\Delta H/RT]$) in order to interpret temperature effect on MB adsorption onto HAp-SA spheres and the calculated thermodynamic parameters were represented in Table 1.

Table 1. *Thermodynamic parameters*

T (^{o}C)	**ΔG (J mole^{-1})**	**ΔH (J mole^{-1})**	**ΔS (J mole^{-1} K^{-1})**
25	-4254	-19316	-50.46
40	-3569		
60	-2489		

Thermodynamic parameters shown in Table 1 specified that the studied adsorption process was exothermic ($\Delta H<0$), decreasing in randomness of adsorbed species ($\Delta S<0$), and spontaneous ($\Delta G<0$).

Equilibrium studies

Adsorption isotherm models are generally evaluated to explain the interaction between adsorbent and adsorbate at adsorption equilibrium, providing the crucial parameter for designing a required adsorption process.

In this study, the linear forms of the Langmuir [$1/q_e = 1/Q^o b(1/C_e) + 1/Q^o$], Freundlich [$\ln q_e = \ln K_f + (1/n)\ln C_e$], and Dubinin–Radushkevich [$\ln q_e = \ln q_m - \beta.\varepsilon^2$] isotherms were applied to the experimental equilibrium data in order to define the adsorption conducts of MB on HAp-SA spheres. The isotherm constants along with regression coefficients (R^2) and error values [$ARE = (100/P)\Sigma(q_{e,cal} - q_{e,exp})/q_{e,exp}$] are shown in Table 2. According to Table 2; the higher R^2 and lower ARE values for Langmuir isotherm model stated that the experimental equilibrium data more fitted to Langmuir model better than the other isotherm models. This case showed that the adsorption of MB onto HAp-SA spheres took place in a homogeneous manner. Many researchers notified the maximum monolayer adsorption capacities of MB for various adsorbents such as 88.89 mg g^{-1} for polydopamine microspheres [6], 94.34 mg g^{-1} for NaAlg-g-poly(AA-co-AAm)/clino hydrogel nanocomposite [7], and 193.16 mg g^{-1} for crosslinked chitosan/bentonite composite [8]. Accordingly; HAp-SA spheres used in this work exhibited significant potential for the MB removal.

Dubinin-Radushkevich (D-R) isotherm model renders possible to designate the type of adsorption, chemical or physical with the aid of the adsorption mean free energy value [$E = 1/(2\beta)^{0.5}$] while Langmuir and Freundlich models do not let take cognizance on adsorption mechanism. D-R isotherm model says that the chemical adsorption process is effective if adsorption energy (E) value is between 8 and 16 kJ mole^{-1} while the physical mechanism prevails for the system if E value is smaller than 8 kJ mole^{-1}, [9]. From Table 2, the calculated energy values for all temperatures were lower than 8 kJ mole^{-1}, which was indicating that the adsorption of MB onto HAp-SA spheres proceeded through physical adsorption.

Table 2. *Adsorption isotherm model parameters*

T (^{o}C)	**Langmuir**				**Freundlich**				**Dubinin-Radushkevich**		
	Q^o	**b**	**R^2**	**ARE**	**K_f**	**1/n**	**R^2**	**ARE**	**q_m**	**E**	**R^2**
20	632.11	0.0030	0.999	8.9412	2.3203	0.8974	0.9655	10.8924	205.02	129.16	0.9763
25	656.59	0.0048	0.9944	7.4559	3.0307	0.9482	0.9831	10.3237	355.20	133.82	0.9894
40	566.25	0.0017	0.9983	4.4528	1.5261	0.8541	0.9782	9.5451	194.47	94.51	0.9849
60	463.82	0.0037	0.9985	14.3455	1.9772	0.8920	0.9236	15.4413	154.74	51.15	0.9921

(Q^o (mg g^{-1}), b (L mg^{-1}), K_f (mg/g(L/mg)$^{1/n}$), q_m (mg g^{-1}), E (J $mole^{-1}$))

Weber-Morris model

For dye adsorption process, dye transfer is frequently described by either external diffusion or intraparticle diffusion or both. Weber-Morris intraparticle diffusion model (q_t=K_i.$t^{0.5}$+I) is the most widely used model for defining the adsorption mechanism. According to Weber–Morris model, if the plot of q_t versus $\sqrt{t}$ gives a straight line and pass through the origin, only intraparticle diffusion is effective on the adsorption process. On the other side, the Weber-Morris plot can be linear and also has intercept value if the adsorption process follows both intraparticle and film diffusion. Also, the slope and intercept values of the model plots of q_t versus $\sqrt{t}$ give intraparticle diffusion rate constants (K_i) and I values related to external mass transfer, respectively. Table 3 shows the Weber-Morris model parameters with regression coefficients for MB adsorption onto HAp-SA spheres.

Table 3. *Weber-Morris model parameters*

Co (mg L^{-1})	**K_i (mg $g^{-1}$$min^{-1/2}$)**	**I**	**R^2**
25	3.244	13.54	0.994
50	4.782	16.26	0.980
75	7.484	27.30	0.993
100	10.84	33.40	0.990
200	15.48	39.60	0.996
300	19.42	44.66	0.998
500	24.49	51.98	0.998

According to Table 3; the internal (K_i) and external (I) diffusion effects gradually increased with increasing initial MB concentration. Weber-Morris model showed that both intraparticle and film diffusion were effective in MB adsorption for HAp-SA spheres.

Fig. 5 represents the comparison of external diffusion effects on MB adsorption for HAp-SA spheres and films. Apparently, plots in Fig. 5 shows multilinearity characterization for the studied adsorption process. The first sharp portion relates to the diffusion of MB through the solution to the external surface of HAp-SA spheres, the second subdued portion is the slow adsorption part, where intraparticle diffusion is rate-controlled, and the last portion represents the adsorption equilibrium [10]. Theoretically, intercept (I) values allow to get information about the thickness of boundary layer, i.e., bigger I value means greater boundary layer effect or external diffusion resistance [11]. Fig. 5 also shows that I value of HAp-SA film is smaller than the sphere one, indicating lower external diffusion resistance of HAp-SA film, which results in early reaching to the equilibrium. As a consequence, the time to reach equilibrium is 60 min for HAp-SA films while it is 240 min for HAp-SA spheres.

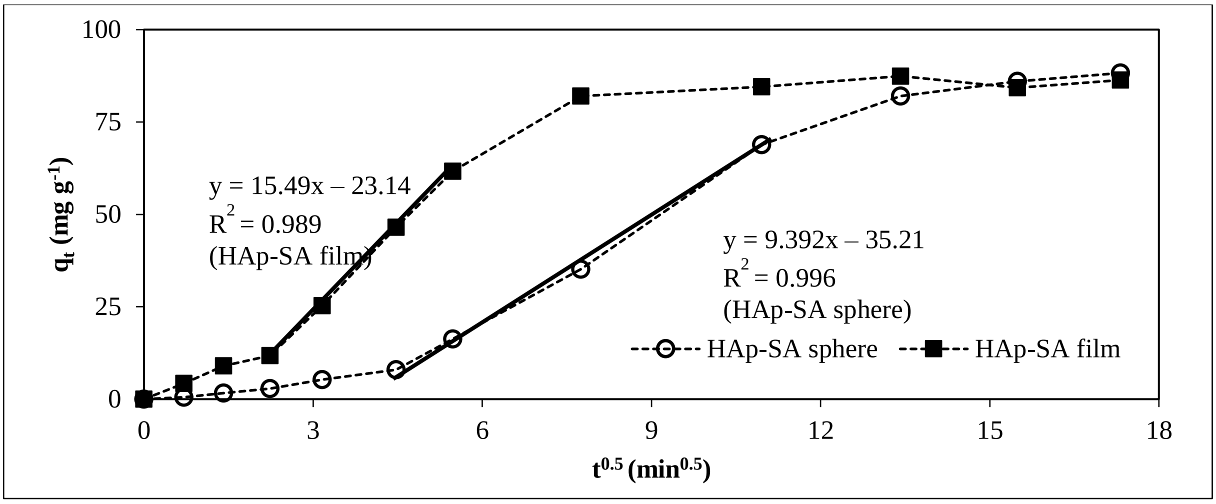

Fig 5. *The comparison of HAp-SA spheres and films (initial pH 9.0, initial dye concentration 100 mg L^{-1}, temperature 25 °C, and adsorbent concentration 1 g L^{-1})*

Adsorbent characterization

HAp-SA spheres, HAp-SA films, SA spheres, and HAp were characterized with FT-IR analysis pre- and post-adsorption, the spectrums are presented in Fig. 6. The HAp spectrum shows absorption bands at 562, 602, 629, 962, and 1026 cm^{-1} corresponding to the PO_4^{3-} ions of the apatite whereas in the HAp-SA spheres and films, the PO_4^{3-} ions appeared at 563, 600, 960, and 1028 cm^{-1}, and at 561, 607, 632, 960, and 1024 cm^{-1}, respectively [12]. In FT-IR spectra of SA, the characteristic peaks of SA can occurred at around 1600 and 1414 cm^{-1} (stretching vibrations of carboxylate), the wide band at about 3300 cm $^{-1}$ (stretching absorption of hydroxyl groups), the bands between 900 and 1200 cm^{-1} (O–C–O stretching of ether groups and –C–O stretching of alcoholic groups), and also the weak peak at 816 cm^{-1} (–Na–O) [13, 14]. The observed bands at 1589 and 1418 cm^{-1} for HAp-SA spheres, 1598 and 1394 cm^{-1} for HAp-SA films suggest that a chemical bond forms between the positive charge of calcium in the inorganic phase (HAp) and the negative charge of the carboxyl group in the organic polymeric matrix (SA) [15].

Besides, FT-IR spectra of MB-loaded adsorbents did not display any significant changes (figure not shown), such as bond breaking or formation, which was indicating that the adsorption processes occurred physically, as determined by D-R isotherm model.

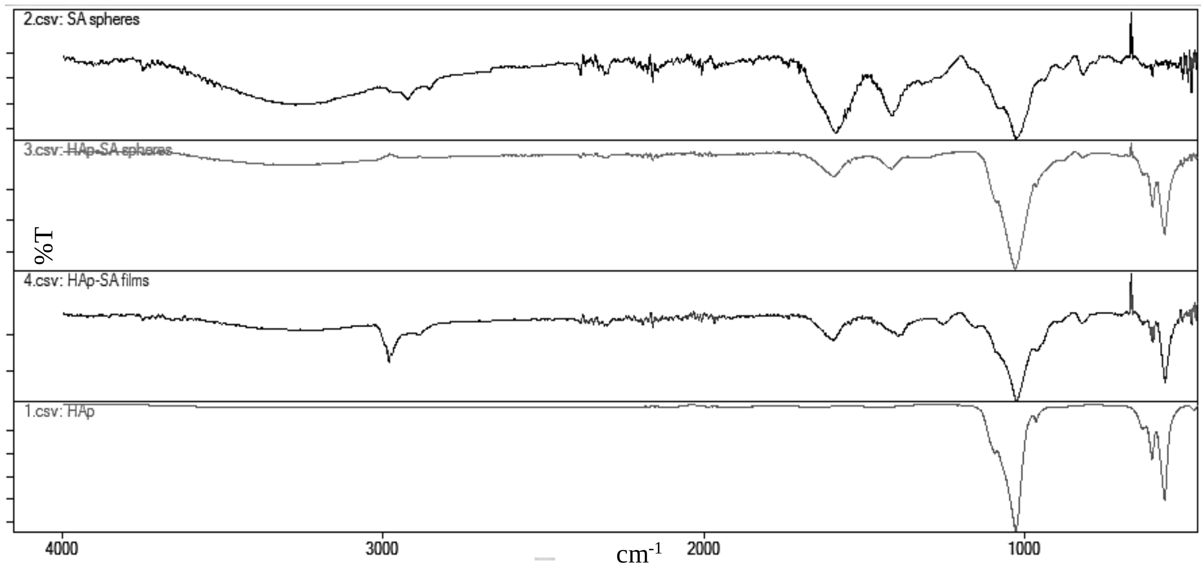

***Fig 6.** FT-IR spectrums of HAp-SA spheres, HAp-SA films, SA spheres, and HAp before adsorption*

Multistage adsorption of MB onto HAp-SA spheres

The dye removal can be attained with major economy of adsorbent if the treatment of dye solution is carried out in separate small batches of adsorbent rather than in a single batch, with filtration between each stage. This system can be established as a multistage equilibrium operation and it is based on equilibrium and a mass balance (Fig. 7).

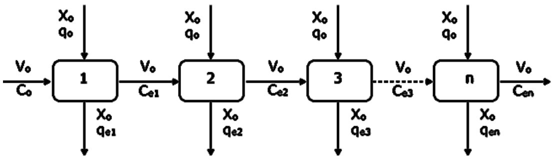

***Fig 7.** Removal process in multistage batch reactors*

The mass balance in the 1st stage is given by Eqn. 1.

$$V_o.C_o + X_o.q_o = X_o.q_{e1} + C_{e1}.V_o \qquad (1)$$

Eqn. 1 can be rearranged as follows,

$$-(V_o/X_o) = (q_{e1}-q_o)/(C_{e1}-C_o) \qquad (2)$$

In the same way, Eqn. 2 can be rearranged for nth stage as follows,

$$-(V_o/X_{(n-1)}) = (q_{en}-q_o)/(C_{e,n}-C_{e(n-1)}) \qquad (3)$$

The adsorbed dye amount per unit mass of adsorbent at the entry in each reactor (q_o) is equal to zero. The operating lines, whose each slope is $-X_o/V_o$, procured from Eqns. (2) and (3), passing through (q_o, C_o) and (q_{e1}, C_{e1}) for the 1st stage and ($q_{e(n-1)}$, $C_{e(n-1)}$) and (q_{en}, C_{en}) for the nth stage, respectively. The parallel operating lines are observed if the adsorbent amounts used in each stage are equal [16].

For MB adsorption onto HAp-SA spheres, the equilibrium curve plotted by the experimental equilibrium data (C_e, q_e) along with the operating lines whose slopes were 1.0 ($-(V_o/X_o)=-(1L/1g)=1$) for three stages were given in Fig. 8. From Fig. 8, for initial MB concentration of 1058.09 mg L^{-1}; the unadsorbed MB amount at the 1th, 2th, 3th, and 4th stages were determined as 537, 162, and 25 mg L^{-1}, respectively.

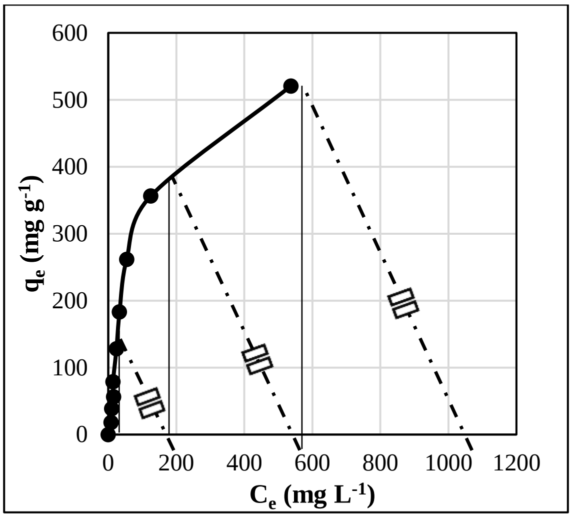

Fig 8. *The equilibrium curve with the operating lines with (V_o/X_o)=-1 for three stages in the multistage batch reactors*

In view of these unadsorbed MB amounts, it is concluded that the three-staged adsorption of MB is required for the desired discharge limits given by Water Pollution Control Regulation of T.R. Environment and Urbanization Ministry (Table 4).

Table 4. *Discharge limit values according to T.R. Environment and Urbanization Ministry*

Parameter	Unit	Sample for 2 hours	Sample for 24 hours
Chemical oxygen demand (COD)	(mg L^{-1})	350	240
Nitrogen of Ammonium (NH_4-N)	(mg L^{-1})	5	-
Free chlorine	(mg L^{-1})	0.3	-
Total chrome	(mg L^{-1})	2	1
Sulfur (S^{-2})	(mg L^{-1})	0.1	-
Sulphite	(mg L^{-1})	1	-
Oil and grease	(mg L^{-1})	10	-
pH	-	6-9	6-9
Color	(Pt-Co) (mg L^{-1})	280 32.2	260 29.9

Conclusions

The experiments of MB adsorption onto HAp-SA spheres were conducted in a single batch mode; the optimum initial pH, initial dye concentration, temperature, and adsorbent concentration were determined to be 9.0, 300 mg L^{-1}, 25 °C, and 1.0 g L^{-1}, respectively. At these optimum conditions; the MB adsorption capacities of HAp-SA spheres, HAp-SA films, alginate spheres, and HAp were determined as 87.89, 83.86, 70.09, and 10.09 mg g^{-1}, respectively. These results show that the envisioned synergistic effect of HAp-SA composite materials could be obtained successfully. The equilibirum studies showed that the maximum monolayer coverage capacity of HAp-SA spheres obtained from Langmuir isotherm model was found as 656.59 mg g^{-1}; besides; the adsorption occurred physically according to E values lower than 8 kJ $mole^{-1}$ computed from D-R isotherm model that also stating exothermic nature of the adsorption. Weber-Morris intraparticle diffusion model showed that both intraparticle and film diffusion were effective in MB adsorption on HAp-SA spheres; and also, HAp-SA films exhibited lower resistance to the external diffusion, which caused to fast equilibrium. The calculated thermodynamic parameters indicated that the adsorption system was exothermic and spontaneous. The adsorbents were characterized with FT-IR analysis, and it was concluded from FT-IR specta post-adsorption that the process was physical adsorption. In addition, the multistage MB adsorption onto HAp-SA spheres was investigated and it was observed that the required discharge limit accepted by T.R. Environment and Urbanization Ministry could be achieved in three-staged adsorption process.

Consequently, the advanced adsorption properties were obtained by synthesizing HAp-SA composite spheres, which could be used effectively for MB removal from aqueous solutions.

Nomenclature

ARE — error value
b — Freundlich isotherm model constant indicated the affinity of the binding sites (L mg^{-1})
C_e — unadsorbed dye concentration at equilibrium (mg L^{-1})
C_{en} — unadsorbed dye concentration at equilibrium for nth stage (mg L^{-1})
C_o — initial dye concentration (mg L^{-1})
E — adsorption energy (kJ mole^{-1})
K_c — adsorption equilibrium constant
K_f — Freundlich isotherm model constant related to adsorption capacity (mg g^{-1})/(L/mg)$^{1/n}$)
K_i — Intraparticle diffusion constant (mg g^{-1} min$^{-0.5}$)
P — number of measurements
R — ideal gas constant (J mole^{-1} K^{-1})
t — time (min)
T — temperature (°C, K)
q_e — adsorbed dye amount per unit mass of adsorbent at equilibrium (mg g^{-1})
q_{en} — adsorbed dye amount per unit mass of adsorbent at equilibrium for nth stage (mg g^{-1})
q_m — maximum adsorption capacity obtained from D-R isotherm model (mg g^{-1})
q_o — adsorbed dye amount per unit mass of adsorbent at the beginning in each reactor (mg g^{-1})
Q^o — maximum monolayer coverage capacity of adsorbent (mg g^{-1})
X_o — adsorbent concentration (g L^{-1})
V_o — volume of adsorption solution (L)
1/n — Freundlich constant stating adsorption intensity
ΔG — Gibb's free energy change (J mole^{-1})
ΔH — enthalpy change (J mole^{-1})
ΔS — entropy change (J mole^{-1} K^{-1})

References

[1] Rao KS, Mohapatra M, Anand S, and Venkateswarlu P, 2010. Review on cadmium removal from aqueous solutions. International Journal of Engineering, Science and Technology, 2.7: 81-103.

[2] Dragan ES (Ed.), 2014. Advanced separations by specialized sorbents (Vol. 108). CRC Press, p. 92.

[3] Ngah WW and Fatinathan S, 2008. Adsorption of Cu (II) ions in aqueous solution using chitosan beads, chitosan–GLA beads and chitosan–alginate beads. Chemical Engineering Journal, 143(1): 62-72.

[4] Googerdchian F, Moheb A, and Emadi R, 2012. Lead sorption properties of nanohydroxyapatite–alginate composite adsorbents. Chemical engineering journal, 200: 471-479.

[5] Mahmoud DK, Salleh MA M, Karim WAWA, Idris A, and Abidin ZZ, 2012. Batch adsorption of basic dye using acid treated kenaf fibre char: equilibrium, kinetic and thermodynamic studies. Chemical Engineering Journal, 181: 449-457.

[6] Fu J, Chen Z, Wang M, Liu S, Zhang J, Zhang J, and Xu Q, 2015. Adsorption of methylene blue by a high-efficiency adsorbent (polydopamine microspheres): kinetics, isotherm, thermodynamics and mechanism analysis. Chemical Engineering Journal, 259: 53-61.

[7] Rashidzadeh A, Olad A, and Salari D, 2015. The effective removal of methylene blue dye from aqueous solutions by NaAlg-g-poly (acrylic acid-co-acryl amide)/clinoptilolite hydrogel nanocomposite. Fibers and Polymers, 16(2): 354-362.

[8] Bulut Y, and Karaer H, 2015. Adsorption of methylene blue from aqueous solution by crosslinked chitosan/bentonite composite. Journal of Dispersion Science and Technology, 36(1): 61-67.

[9] Chowdhury S, Mishra R, Saha P, and Kushwaha P, 2011. Adsorption thermodynamics, kinetics and isosteric heat of adsorption of malachite green onto chemically modified rice husk. Desalination, 265(1): 159-168.

[10] Wang H, Yuan X, Wu Y, Huang H, Zeng G, Liu Y, and Qi Y, 2013. Adsorption characteristics and behaviors of graphene oxide for Zn (II) removal from aqueous solution. Applied Surface Science, 279: 432-440.

[11] Tan IA, Ahmad AL, and Hameed BH, 2008. Adsorption of basic dye on high-surface-area activated carbon prepared from coconut husk: Equilibrium, kinetic and thermodynamic studies. Journal of hazardous materials, 154(1): 337-346.

[12] Sivakumar M, and Rao KP, 2003. Preparation, characterization, and in vitro release of gentamicin from coralline hydroxyapatite-alginate composite microspheres. Journal of Biomedical Materials Research Part A, 65(2): 222-228.

[13] Rashidzadeh A, and Olad A, 2014. Slow-released NPK fertilizer encapsulated by NaAlg-g-poly (AA-co-AAm)/MMT superabsorbent nanocomposite. Carbohydrate polymers, 114: 269-278.

[14] Dhanapal V, and Subramanian K, 2014. Recycling of textile dye using double network polymer from sodium alginate and superabsorbent polymer. Carbohydrate polymers, 108: 65-74.

[15] Pandi K, and Viswanathan N, 2014. Synthesis of alginate bioencapsulated nano-hydroxyapatite composite for selective fluoride sorption. Carbohydrate polymers, 112: 662-667.

[16] Özer A, Özer D, Dursun G, Bulak S, 1999. Cadmium (II) adsorption on Cladophora crispata in batch stirred reactors in series. Waste Management, 19(3): 233-240.